Fachtagung "Experimentelle Strömungsmechanik"
7.–9. September 2021, Bremen

Transsonische Strömungs-Struktur-Interaktion: Bestimmung der „Buffeting"-Grenzen eines superkritischen Flügelprofils mit einem Nick-Freiheitsgrad

Transonic fluid-structure interaction: determination of "buffeting" boundaries of a supercritical airfoil with a pitching degree of freedom

Tim Baur, Alessandro Accorinti, Sven Scharnowski, Christian J. Kähler
Institut für Strömungsmechanik und Aerodynamik, Universität der Bundeswehr München,
Werner-Heisenberg-Weg 39, 85577 Neubiberg

Strömungs-Struktur-Interaktion, Buffeting, transonische Strömungen, Aeroelastik
Fluid-structure interaction, buffeting, transonic flows, aero-elasticity

Abstract

The transonic flow around a supercritical airfoil was investigated in order to gain better knowledge of the root-cause of buffet and the corresponding fluid-structure interaction. For that purpose, an experimental setup for the Trisonic Wind Tunnel Munich was designed and manufactured. The design is integrating a rigid supercritical airfoil (OAT15A) with a pitching degree of freedom. Preceding the detailed investigation of the underlying physical mechanisms of the phenomenon, a detailed analysis of the buffet(-ing) boundaries with respect to flow and structural parameters is crucial. Therefore, pre-buffet and buffet flows were analyzed by changing Mach number and angle of attack. Structural properties were varied by modifying spring stiffness and moment of inertia. High-speed background-oriented Schlieren measurements were used to observe the shock with its dynamics. A high-speed stereo camera setup for correlation-based deformation measurements was implemented to track the dynamics of the structural motion.

An extensive dataset for varying flow and structural parameters and the corresponding intensity of fluid-structure interaction could be obtained. A safe operation of the airfoil at partially severe flutter conditions was achieved. Dominant frequencies and amplitudes of structural and fluid modes were extracted, allowing the identification of regions of independent and locked-in mode presence, as well as critical resonance. For this article, one exemplary run, exhibiting classical bending-torsion flutter with limit-cycle oscillations, was selected as to present the experiment and the data analysis approach.

Introduction

The development and operation of modern commercial aircraft is strongly driven by the demand for high cost- and fuel efficiency. As for cost-efficiency, the increase of flight speed is a crucial parameter. At the common, high subsonic cruise speed, local velocities on a supercritical airfoil can exceed sonic boundaries and lead to a supersonic flow region on the airfoil suction side. This local region is terminated by a shock wave, leading to a sudden flow deceleration and pressure increase, to satisfy the subsequent higher static pressure boundary conditions of the main flow. Depending on the shock strength, boundary layer separation may occur. At

increasing flight speeds or angles of attack (AoA), the shock wave can become unstable and result in an oscillating shock-wave-boundary-layer interaction. This phenomenon is denoted as transonic shock buffet (McDevitt and Okuno. 1985, Jacquin et al. 2009, Accorinti et al. 2020). Due to the associated strong load variations and possible interaction with the structure, it is the principal limiting factor of the flight envelope of modern commercial aircraft. (Badcock et al. 2011, Gao and Zhang. 2020). Transonic buffet has been studied over decades but a comprehensive physical explanation of the root-cause remains missing. Multiple hypotheses and observations have been published offering explanation and prediction of the buffet boundaries (onset and offset) for different combinations of airfoil shapes and operating conditions. Besides the already mentioned involved interaction between shock wave and boundary layer, a pressure-driven feedback from other regions around the airfoil is assumed by multiple researchers to be involved in the creation of the instability (Lee 2001, Feldhusen-Hoffmann et al. 2021). The association of buffet as a global flow instability (Crouch 2009) also declared as an unstable fluid mode, based on flow Eigenvalue analysis, has been widely accepted (Gao and Zhang. 2020, Giannelis et al., 2020).
If the Eigenfrequencies of the wing structure are of the same order of magnitude as the shock buffet frequency, the phenomenon can induce a structural response, which is commonly known as “buffeting”. This self-excited fluid-structure interaction (FSI) results in a limitation of fatigue life of the aircraft, eventually even in catastrophic structural failure. Furthermore, the latest numerical research in the field of transonic aeroelasticity indicates an influence of structural characteristics on the flow stability boundary and states the necessity of always simulating buffeting as fluid-structure coupled system with structural feedback, rather than a unidirectional system. In that case, the rigid-wing buffet is only the boundary case for an infinitely stiff structural system (Gao and Zhang. 2020, Nitzsche et al. 2019).
Given this variety of open questions and the latest findings in the field, which are mainly based on numerical research, experimental data is needed to back them up. Therefore, an experimental setup was designed to investigate the phenomenon, with particular attention to the self-excitation of transonic FSI. After an extensive measurement campaign with focus on buffet onset boundaries on a rigid, zero degree-of-freedom (0DOF) wing, the pitching degree of the wing was released, and the torsional spring stiffness adjusted to reach a pitching Eigenfrequency in the vicinity of shock buffet.
The focus of this study was to generate safe experiments at a set Mach number while approaching the flutter boundaries by increasing the AoA. Optical measurement techniques were deployed to allow the non-intrusive observation of fluid and structural modes and, hence, the detection of the instability and interaction boundaries. The following sections discuss the experimental setup and facility, followed by detailed information about the optical techniques and image analysis. The presentation of results is followed by a summary, concluding remarks and future aspects of the presented work.

Experimental setup

The experiments were perfomed in the Trisonic Wind Tunnel of the Bundeswehr University in Munich (TWM). It is a blow-down type wind tunnel with a rectangular test section of 300 mm width and 680 mm height and allows for aerodynamic profile testing from subsonic to supersonic flows with total pressures up to 5 bar. A detailed description of the facility can be found in Bolgar et al. 2018. Boundary layer growth in the test section was compensated through diverging horizontal walls and by using boundary layer suction on the vertical walls. The divergence and suction settings were optimized in advance to obtain a constant pressure distribution throughout the empty test section in streamwise direction for all relevant Mach numbers.

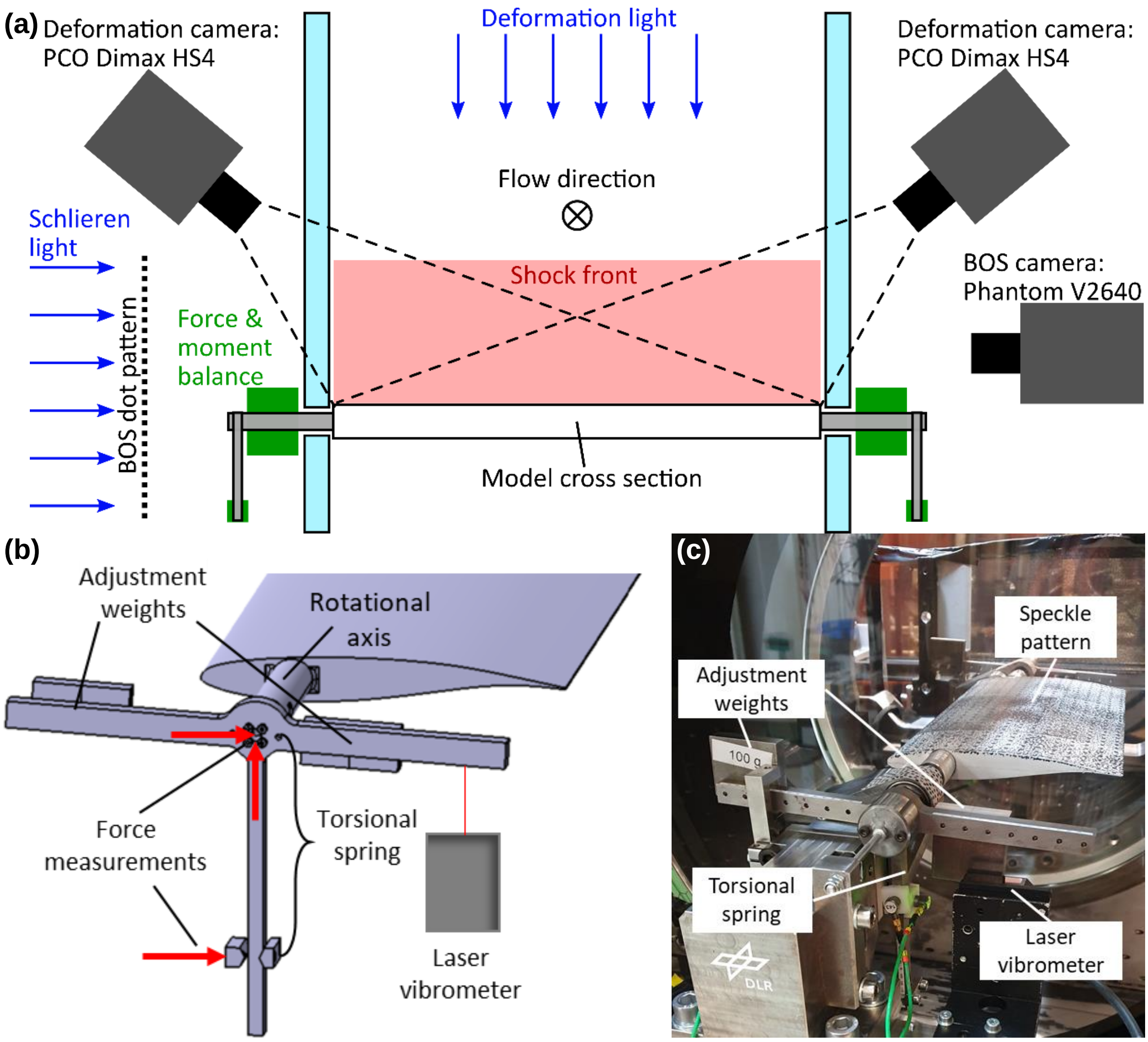

Fig. 1: a) Front view of the measurement setup. b) Sketch and c) photo of the structural implementation of the spring-mounted rigid wing with a pitching degree of freedom.

The tested OAT15A airfoil introduced a maximum blockage of 3.5% at the highest AoA considered. Fig. 1 shows the experimental setup for the operation of flutter experiments with a single degree of freedom. Focus of the design was the spring-mounted pitching degree of freedom allowing simultaneous 3D-force and aerodynamic moment measurements on either wing side while maintaining optical access. The rectangular OAT15A wing model, manufactured from carbon-fiber reinforced plastics has a span of 298 mm and chord of c = 150 mm. The boundary layer was tripped at 7% of chord on both, suction, and pressure side, by a dotted line of circular stickers of 3 mm diameter and 60 µm thickness at 6 mm distance. An integrated steel shaft, located at 25% of chord, defined the rotational axis. An externally attached set of lever arms and adjustment weights undertook the role of the torsional spring and allowed the adjustment of moment of inertia and center of gravity. Laser-vibrometer measurements on one lever arm were used to complement the force measurements with online information about the current amplitude and frequency content of the pitching motion. A mechanical stop was used to limit the model pitching motion to a maximum of ±1.5° of AoA. Approaching this limit, an automatic alarm signal based on the laser vibrometer, gave an indication to interrupt the wind tunnel runs before exposing model and setup to excessive (fatigue) loads or causing structural failure.

Optical measurement techniques

For the non-intrusive measurements of the shock wave position and its fluctuations, spanwise background-oriented Schlieren (BOS) measurements were deployed. A random point-like pattern was positioned in the background of the test section and illuminated from the back with parallelized light of a blue LED (Luminus CBT-120-B-C11KM301, 462 nm). Images of the pattern were recorded from the opposite side by a Phantom V2640 high-speed camera with an image rate of 1000 Hz (see Fig. 1). Density gradients and the corresponding change of refraction index led to a distortion of the dot pattern that allowed for a qualitative reconstruction of the density gradients in the flow by spatial cross-correlation with an undisturbed reference image, as discussed in Raffel 2015. Fig. 2a) shows a raw image of the test section with clear presence of a shock wave. In Fig. 2b) the resulting displacement map of the cross-correlation is displayed. Furthermore, the results of an algorithm-based detection of the shock-position at different heights of the wing surface are visualized by means of black circles in the figure.

Structural deformations of the wing were detected via stereo digital image correlation (DIC) measurements (Hijazi and Kähler, 2017). A random speckle pattern was applied to the upper wing surface to optimize the correlation results. The pattern was illuminated from the top of the test section by four UV-LEDs (Luminus CBM-120-UVX, 410 nm). Two high-speed cameras (PCO Dimax HS4), mounted outside the test section side windows, observed the suction side under an angle of approx. 30°. Images were recorded synchronously with a recording rate of 1000 Hz. Making use of an a priori coplanar volume calibration of the stereo camera setup, a correlation-based 3D surface reconstruction was performed for every image pair. In Fig. 2c) an example result of the obtained deformation field with respect to wind-off conditions at a Mach number of 0.74 and an AoA of 6.0° can be seen. The results clearly show the presence of three-dimensional wing deformations, constituted of a span wise bending, resulting in higher

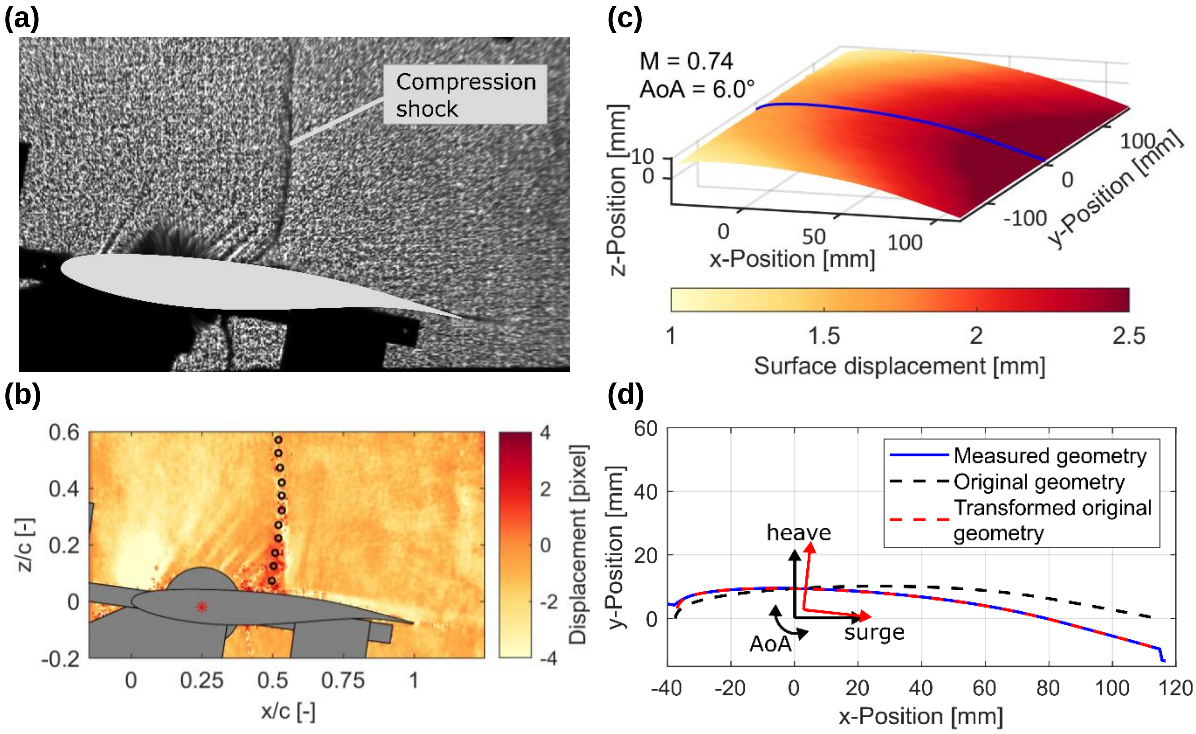

Fig. 2: a) Raw image of background-oriented Schlieren measurements exhibiting a shock on the airfoil suction side. b) Correlation-based, surface tangential displacement field. c) Surface displacement field at Mach number 0.74 and an AoA of 6°. d) Sketch of contour fitting algorithm: Measured surface contour at wing center (blue), OAT15A original contour at zero AoA (black) and fitted geometry (red) with resulting AoA, vertical and streamwise shift, heave and pitch, respectively.

GALA e.V., Karlsruhe, Germany, ISBN 978-3-9816764-7-1

displacements in the wing center, and a torsion around the elastic axis, that leads to higher displacements towards the trailing edge. As to separate the two effects, the cross section for each span wise position was extracted and analyzed using an airfoil-shape-fitting algorithm (see Fig. 2d)). The obtained span wise distribution of local AoA, vertical and streamwise displacement (heave and surge), showed average variations below 0.05°, 0.5 mm and 0.2 mm, respectively. Based on this indication of a sufficiently rigid structure, the actual AoA and shift values extracted from the center cut (depicted in blue in Fig. 2c)) were used as the reference values for further evaluation.

Experimental results

Due to limited camera memory, each measurement was restricted to a duration of 13 s. During that time, the prescribed AoA of the facility was continuously increased from 3° to 7°, simultaneously increasing the blockage and reducing the initial Mach number, in case of the presented run from M = 0.752 to 0.744. The total pressure was set to 1.5 bar resulting in a chord-based Reynolds number of approx. 3 x 10^6 for the given Mach number range. The pitching moment of inertia was adjusted to obtain a pitching Eigenfrequency of f_θ = 101 Hz, corresponding to a reduced frequency range from $k_\theta = (\pi f_\theta c) / U$ = 0.194 to 0.199, where U is the inflow velocity decreasing from 244.9 to 239.7 m/s. Given the fluid mode (buffet) Eigenfrequency obtained from Accorinti et al. 2021, of $f_b \approx$ 97 Hz (k_b = 0.192), an intense FSI was expected. The center of gravity of the moving parts was adjusted to coincide with the elastic axis to avoid and reduce any coupling between structural modes at wind-off and wind-on conditions, respectively.
For the evaluation, the prescribed AoA sweep was divided into intervals of 0.1° for which statistics and frequency content were analyzed. Fig. 3a) shows the time average of the measured AoA with its standard deviation versus the prescribed wind tunnel AoA. Due to static structural deformation of the torsional spring and shaft a prescribed AoA lead to a constantly diminished measured AoA, reduced by approx. 1.5°. Therefore, all results are referring to the actual AoA instead of the prescribed one. Starting from an AoA of 4.6° a strong increase of fluctuations of the measured AoA can be observed, showing the clear presence of a strong pitch motion. It reaches a maximum level at 4.9° that remains up to the maximum tested incidence, indicating limit cycle oscillations (LCO). It must be noted, that despite a strong shock presence and resulting boundary layer separation, the static deformation and therefore, the aerodynamic moment, remains constant (constant slope). The results of spectral analysis of the AoA for each interval are presented in Fig. 3b). Despite the partially low quality of the spectra based on the limited number of samples, dominant regions can be identified clearly. These are, a less prominent region around f_θ = 380 Hz, that might be connected to wind-tunnel pressure fluctuations, and the more prominent region from f_θ = 110 to 115 Hz associated with an increased structural Eigenfrequency due to coupling between pitch and heave. Together with the sudden onset of fluctuations, the peak height of the dominant frequency indicates flutter onset. Fig. 3e) and f) show the corresponding results for the heave (vertical) motion of the wing. Negative values are attributed to a shaft mounting position below the coordinate system origin. By this, a free shaft motion even at higher average heave values, resulting from less structural stiffness of the shaft outside the wing, was allowed. Up to an AoA of 4.5°, a constant increase of vertical displacement with low fluctuations was observed. The separation of the boundary layer interrupts the increase of the lift and, consequently, of the average displacement. The corresponding frequency spectrum shows dominant but weak regions at approx. 130 Hz, 225 Hz (coupled structural heave and surge mode) and 170 Hz (structural heave Eigenfrequency). Similarly to the pitching, starting from 4.6° an onset of strong fluctuations and a highly dominant frequency peak at f_h = 110 Hz is visible and indicates strong coupled pitch-heave motion. In Fig. 3c) and d), the evaluation of the shock position with respect to the AoA can be seen. Starting from an

AoA of 2.5° a reliable shock detection seems to be possible (reduced fluctuations), and a downstream motion of the shock can be observed. The shock motion inversion point, indicating boundary layer separation, and necessary criterion for buffet onset (Crouch et al. 2009), is reached at 4.3°. A slight upstream motion of the shock is followed by a strong increase of fluctuations at approx. 4.7° that remain on a constant level. The frequency spectra do not exhibit any dominant peaks before the onset, starting from which, also higher harmonics of the strongly dominant frequency of f = 110 to 115 Hz can be identified.

In the presented case the most dominant peaks of both, structural and fluid modes, are of the same frequency and coincident onset-AoA. Most obviously, a classical bending-torsion flutter has been generated (Gao and Zhang. 2020). In order to detect less obvious interaction regions, cross-correlation of fluid and structural signals are applied. In Fig. 3g) and h) one can see the

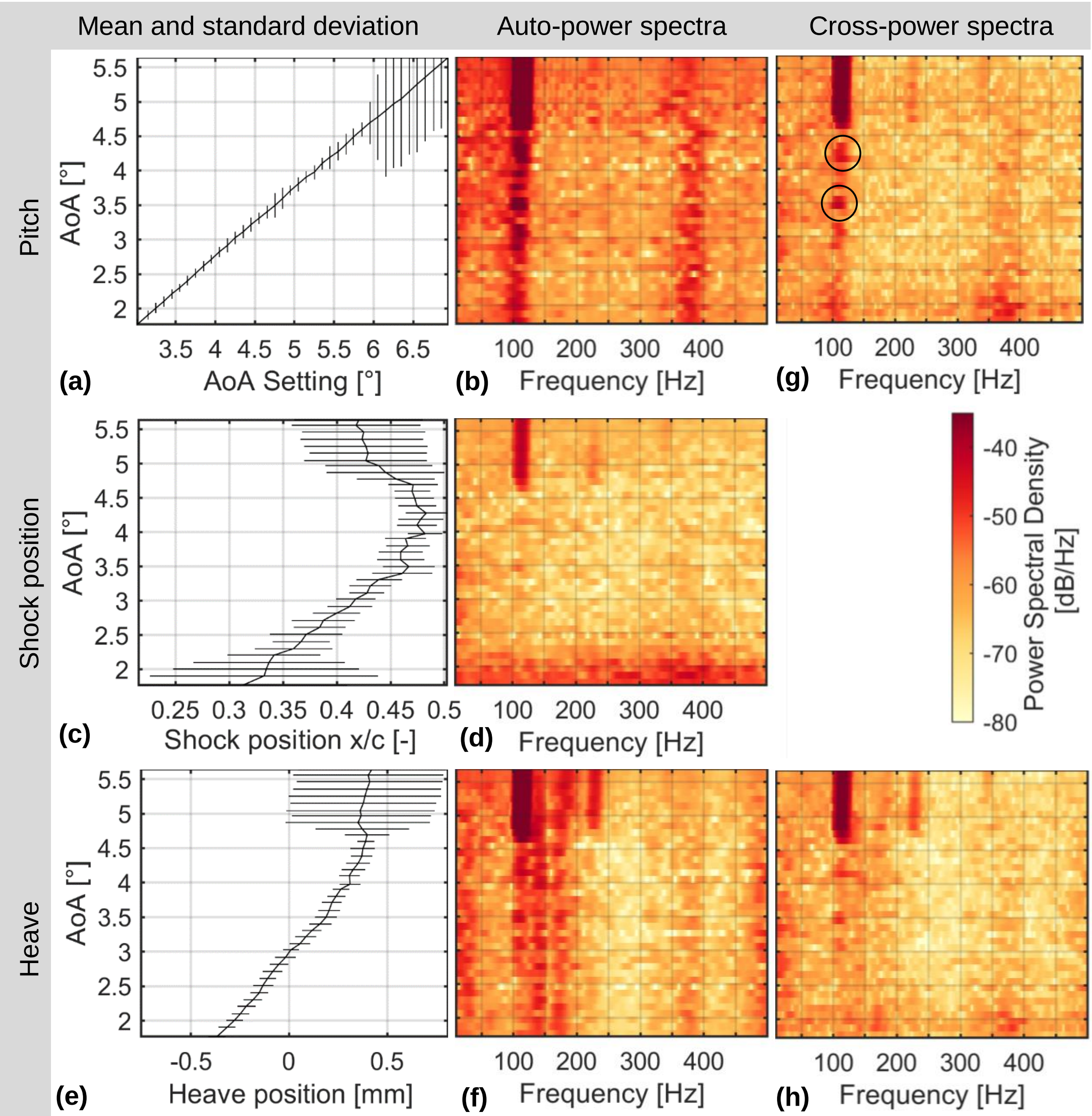

Fig. 3: Interval-based evaluation of an AoA sweep at an initial Mach number M = 0.752 (decreasing to 0.744) with an AoA interval size of 0.1°. a), c) and e) show mean values and standard deviations for the given intervals b), d) and f) represent the auto power spectra for pitch angle, shock position and heave position, respectively. g) and h) display the cross power spectra of the signals of shock position cross-correlated with pitch angle and heave position, respectively.

cross-correlated power spectral density for the combined signals of shock position with pitch and heave, respectively. The strongly coupled buffeting regions remain clearly visible. However, other regions, possibly of interaction between shock and structure, are now allocatable, as marked by the black circles in Fig. 3g). The physical explanation of these remains elusive at this point. Furthermore, cross-correlations between structural signals allow the identification of occurring mode shapes (e.g., cross-correlation of pitch with heave signal shows peaks where coupled motion occurs).

Summary and conclusions

For the ultimate goal of a detailed investigation of “buffet” and its concurring FSI “buffeting”, an experimental wind-tunnel setup was designed, manufactured and tested. The spring-mounted wing (OAT15A) with a pitching degree of freedom allows for a variation of structural parameters as spring stiffness and moment of inertia. Wind-tunnel runs in the transonic regime were performed, increasing the AoA at a Mach number that decreased slightly with increasing AoA due to blockage. The exemplary run presented in this article exhibited strong harmonic FSI at higher AoA with limited amplitudes (LCO). High-speed optical measurement techniques, BOS and deformation, were deployed to non-intrusively observe structural and fluid modes. Subsequent image processing and analysis allowed for the extraction of shock position, pitching angle and heave position of the wing, which facilitated the separation of the superimposed span wise bending and rotation of the structure. A constant aerodynamic moment, based on a constant static rotational deformation could be observed throughout the whole AoA sweep. The constant increase of lift-based wing bending was interrupted once the region of strong FSI was reached, supposedly coinciding with boundary layer separation. At higher AoA, a strong increase of fluctuations of pitch, heave and shock position was observed implying a coupled FSI, categorized as classical bending-torsion flutter. The desired limitation of structural motion to only one degree of freedom (pitch) was not fulfilled, however, amplitudes of other degrees of freedom could be restrained to a low level. Further increase of AoA did not lead to stronger fluctuations, indicating constant amplitudes and, hence, LCO. Interval-based frequency analysis confirmed the existence of harmonic shock and structural oscillations that occurred at a higher frequency than in the rigid case, arguably based on the influence of structural coupling of pitch and heave mode. Cross-power spectra, created from the time signals of the shock position and the structural motions, respectively, enabled a more distinct visualization of coupled regions and the corresponding dominant frequencies. The observation of intermitting interaction regions below the onset-AoA with strong fluctuations implies that additional unexpected FSI could have occurred.

Given the presented experimental setup, measurement techniques and the subsequent evaluation methods a successful, safe FSI measurement campaign could be conducted. Furthermore, it will allow for a detailed investigation of the underlying physical mechanisms of “buffeting”. Subject to upcoming studies will be parametric variations of structural and further fluid parameters (spring stiffness, moment of inertia, Mach numbers, AoA) that will give deeper insight into the parametric dependencies of the FSI on- and offset boundaries. Additionally, other optical measurement techniques, like particle image velocimetry (PIV) and pressure sensitive paint (PSP) will be used to investigate the role of boundary layer and pressure field dynamics within the FSI.

Acknowledgements

Financial support in the frame of the project HOMER (Holistic Optical Metrology for Aero-Elastic Research) from the European Union's Horizon 2020 research and innovation program under grant agreement No. 769237 is gratefully acknowledged. Furthermore, the authors like to thank Jens Nitzsche, Yves Govers, Johannes Dillinger, Johannes Knebusch and Tobias Meier from the DLR Institute of Aeroelasticity for their contribution and expertise in design, manufacturing and integration of the presented setup.

References

Accorinti, A., Baur, T., Scharnowski, S., Knebusch, J., Dillinger, J., Govers, Y., Nitzsche, J., Kähler, C.J., 2021:"Measurements of deformation, schlieren and forces on an OAT15A airfoil at pre-buffet and buffet conditions", IOP Conference Series: Materials Science and Engineering, Vol. 1024, p. 012052, DOI: 10.1088/1757-899x/1024/1/012052

Badcock, K.J., Timme, S., Marques, S., Khodaparast, H., Prandina, M., Mottershead, J.E., Swift, A., Ronch, A.D., Woodgate, M.A., **2011**: "Transonic aeroelastic simulation for instability searches and uncertainty analysis", Progress in Aerospace Sciences, Vol. 47, No. 5, pp. 392-423

Bolgar, I., Scharnowski, S., Kähler, C.J., 2018: "The Effect of the Mach Number on a Turbulent Backward-Facing Step Flow", Flow, Turbulence and Combustion, Vol. 101, No. 3, pp. 653-680

Feldhusen-Hoffmann, A., Lagemann, C., Loosen, S., Meysonnat, P., Klaas, M., Schröder, W., 2021: "Analysis of transonic buffet using dynamic mode decomposition", Experiments in Fluids, Vol. 62, No. 4, p. 66

Gao, C., Zhang, W., 2020: "Transonic aeroelasticity: A new perspective from the fluid mode", Progress in Aerospace Sciences, Vol. 113, p. 100596

Giannelis, N.F., Levinski, O., Vio, G.A., 2020: "Origins of atypical shock buffet motions on a supercritical aerofoil", *Aerospace Science and Technology*, Vol. 107, p. 106304

Hartmann, A., Feldhusen, A., Schröder, W., 2013: "On the interaction of shock waves and sound waves in transonic buffet flow", *Physics of Fluids*, Vol. 25, p. 026101

Hijazi, A., Kähler, C.J., 2017: "Contribution of the Imaging System Components in the Overall Error of the Two-Dimensional Digital Image Correlation Technique", *Journal of Testing and Evaluation*, Vol. 45, No. 2, p. 20150437

Jacquin, L., Molton, P., Deck, S., Maury, B., Soulevant, D., 2009: "Experimental Study of Shock Oscillation over a Transonic Supercritical Profile", *AIAA Journal*, Vol. 47, Sep, pp. 1985-1994

Lee, B.H.K., 2001: "Self-sustained shock oscillations on airfoils at transonic speeds", *Progress in Aerospace Sciences*, Vol. 37, pp. 147-196

McDevitt, J.B., Okuno, A.F., 1985: "Static and dynamic pressure measurements on a NACA0012 airfoil in the Ames high Reynolds number facility", NASA Technical Paper, No. 2485

Nitzsche, J., Ringel, L., Kaiser, C., Hennings, H., 2019: "Fluid-mode flutter in plane transonic flows", IFASD 2019 – International Forum on Aeroelasticity and Structural Dynamics

Pearcey, H.H., 1955: "Some effects of shock-induced separation of turbulent boundary layers in transonic flow past aerofoils", A.R.C. Technical Report: Reports and Memoranda, No. 3108

Raffel, M., 2015: "Background-oriented schlieren (BOS) techniques", Experiments in Fluids, Vol. 56

Zhou, T., Dowell, E., Feng, S.S., 2019: "Computational investigation of wind tunnel wall effects on buffeting flow and lock-in for an airfoil at high angle of attack", Aerospace Science and Technology, Vol. 95, p. 105492